EINDHOVEN UNIVERSITY OF TECHNOLOGY

Mode reduction applied to initial post-buckling behavior

Citation for published version (APA):
Schreppers, G-JMA., & Menken, C. M. (1994). Mode reduction applied to initial post-buckling behavior. In G. M. A. Kusters, & M. A. N. Hendriks (Eds.), *DIANA computational mechanics : 1st international conference on computational mechanics : proceedings, Delft, 1994* (pp. 287-296). Kluwer Academic Publishers.

Document status and date:
Published: 01/01/1994

Document Version:
Publisher's PDF, also known as Version of Record (includes final page, issue and volume numbers)

Please check the document version of this publication:

• A submitted manuscript is the version of the article upon submission and before peer-review. There can be important differences between the submitted version and the official published version of record. People interested in the research are advised to contact the author for the final version of the publication, or visit the DOI to the publisher's website.
• The final author version and the galley proof are versions of the publication after peer review.
• The final published version features the final layout of the paper including the volume, issue and page numbers.

Link to publication

General rights
Copyright and moral rights for the publications made accessible in the public portal are retained by the authors and/or other copyright owners and it is a condition of accessing publications that users recognise and abide by the legal requirements associated with these rights.

• Users may download and print one copy of any publication from the public portal for the purpose of private study or research.
• You may not further distribute the material or use it for any profit-making activity or commercial gain
• You may freely distribute the URL identifying the publication in the public portal.

If the publication is distributed under the terms of Article 25fa of the Dutch Copyright Act, indicated by the "Taverne" license above, please follow below link for the End User Agreement:

www.tue.nl/taverne

Take down policy
If you believe that this document breaches copyright please contact us at:

openaccess@tue.nl

providing details and we will investigate your claim.

Download date: 04. Oct. 2023

MODE-REDUCTION APPLIED TO INITIAL POST-BUCKLING BEHAVIOR

G.M.A. SCHREPPERS
TNO Building and Construction Research, The Netherlands

and

C.M. MENKEN
Eindhoven University of Technology, Department of Mechanical Engineering

Abstract This paper presents a perturbation approach for analyzing the (initial) post-buckling behavior of elastic structures. In this perturbation a small number of buckling modes is taken into account. This approach results in a potential energy function which is defined in terms of amplitudes of the selected modes. The post-buckling displacement field is solved from the reduced set of equilibrium equations where the unknowns are the amplitudes of the Euler modes which are selected for the asymptotic expansion. To perform this technique the segment PERTUR in module *EULER is designed in DIANA 6.0. The theory of this segment and two calculating examples are demonstrated.

1. Introduction

In general the equilibrium paths of thin-walled structures are capricious and may show limit points with very strong curvatures as well as bifurcation points. Because of these strong nonlinearities the incremental approach requires a large number of steps. In order to keep the calculation time acceptable, mode-reduction is applied to the full system of discretized equations. Further, the complex character of these structures, which is generally difficult to predict, can be made more accessible for better understanding, when the technique of mode-reduction is applied. Koiter [4] was the first one formulating the perturbation approach for initial post-buckling analysis of continua. His theory considers conservative systems exhibiting bifurcational buckling in the perfect case. The approach does not allow for any physical nonlinearities, while geometrically nonlinear effects are only taken partly into account. Such as Koiter already noticed the range of validity of this approach around the critical point may be quite small. In the particular case that the fundamental path has a cluster of bifurcation points just above the critical point, this may be a serious limitation. In this case the respective buckling modes usually exhibit a strong coupling to each other. These interaction effects should be taken into account by considering the quadric and the cubic terms of the potential energy function. The approach presented here is based on the formulation of Byskov and Hutchinson [1] which is in fact a modification of the formulation of Koiter. In this approach there is no limitation on the distance between the critical points. In the post-buckling displacements however, it remains an asymptotic theory. Therefore, this method may be considered to have a wider range of application than the original approach presented by Koiter. However, there is no method known to ascertain the range of validity for this approach. The mode-interaction is an essential aspect in the presented approach and therefore the second-order fields must be calculated. In comparison to the wave-shaped deformations

G.M.A. Kusters and M.A.N. Hendriks (eds.), DIANA Computational Mechanics '94, 287-296.
© 1994 *Kluwer Academic Publishers. Printed in the Netherlands.*

which occur in the buckling modes, the according second-order fields show waves with the half wave-length. This property brings extra requirements with respect to the fineness of the mesh-distribution. The combination of the mesh-distribution and the elemental interpolation-functions must be suitable for describing the highly frequency wave shapes of the second-order fields. For this special purpose elements with spline-function interpolation are developped and applied in the examples underneath. The numerical application of the theory can be used very suitable if there are not to many critical points in between the relevant ones. A class of applications to which this may be of special interest are e.g. the stiffened panels in aeronautical structures and prismatic profile beams which can be used for construction of glasshouses.

2. Theory

The set of equations representing nodal equilibrium is written as

$$\mathbf{r}(\mathbf{u})=\mathbf{f}(\mathbf{u}) \tag{1}$$

where $\mathbf{r}$ represents the internal force vector, $\mathbf{f}$ the external force vector and $\mathbf{u}$ represents the vector of nodal degrees of freedom (displacements). A critical point is identified with the vanishing of quadratic terms in the potential energy function. $\mathbf{u}^{crit}$ is a critical point in the space of possible displacement vectors and defined by the equation of nodal equilibrium

$$\mathbf{r}(\mathbf{u}^{crit}+\delta\mathbf{u})=\mathbf{f}(\mathbf{u}^{crit}+\delta\mathbf{u}) \tag{2}$$

which must be valid for arbitrary 'small' $\delta\mathbf{u}$. Suppose a solution $\mathbf{u}^{lin}$ from the linearized equilibrium equation is known, i.e. $\mathbf{u}^{lin}$ resulting from

$$\mathbf{K}_L\,\mathbf{u}^{lin}=\mathbf{f} \tag{3}$$

where $\mathbf{K}_L$ is the linear stiffness-matrix, with $\mathbf{K}_G$ being the geometrical stiffness-matrix, critical points may be calculated by solving the condition

$$\det(\mathbf{K}_L+\lambda\,\mathbf{K}_G(\mathbf{u}^{lin}))=0 \tag{4}$$

where λ is the load-parameter. The purpose of perturbation analysis is to calculate a post-buckling displacement field $\mathbf{u}^{pb}$ satisfying the equilibrium condition but $\mathbf{u}^{pb}$ being different from the primair path $\mathbf{u}=\lambda\,\mathbf{u}^{lin}$. It is assumed that there are M coinciding or nearly coinciding interacting modes. In consistancy with the DIANA Manual these modes which will be noted by ϕ_k, $k=1,\ldots,M$. The initial post-buckling displacement field $\mathbf{u}^{pb}$ is defined to be

$$\mathbf{u}^{pb}\;=\;\lambda\,\mathbf{u}^{lin}+a_i\,\phi_i+a_i\,a_j\,\mathbf{u}_{ij} \tag{5}$$

where $\mathbf{u}_{ij}$ is called the second-order field, and each a_i is the amplitude of the respective mode ϕ_i. In literature [3] it is shown that $\mathbf{u}_{ij}$ must be calculated by solving the equation

$$(\mathbf{K}_L+\lambda_p\,\mathbf{K}_G(\mathbf{u}^{lin}))\,\mathbf{u}_{ij}=\mathbf{f}_{ij} \tag{6}$$

applying to the orthogonality conditions

$$(\phi_k)^T\,\mathbf{K}_L\,\mathbf{u}_{ij}=0,\qquad k=1,\ \ldots,\ M \tag{7}$$

where $\mathbf{f}_{ij}$ is defined as the mode interaction load vector

$$\mathbf{f}_{ij} = \int_{V_0} (\mathbf{B}_L^T \sigma_{ij} + \mathbf{B}_{NL}^T (\phi_i) \sigma_j + \mathbf{B}_{NL}^T (\phi_j) \sigma_i) \, dV_0 \quad (8)$$

with σ_{ij} being the stresses related to the interaction of modes i and j, σ_i being the stresses related to mode i, $\mathbf{B}_L$ being the linear strain-displacement matrix and $\mathbf{B}_{NL}$ being the nonlinear strain-displacement matrix. Further, the energy potential can now be written as a function of the load-parameter λ and the mode amplitudes a_i :

$$P(a_i, \lambda) = \frac{1}{2} \sum_{I=1}^{M} (1 - \frac{\lambda}{\lambda_I}) a_I a_I + A_{ijk} a_i a_j a_k + A_{ijkl} a_i a_j a_k a_l \quad (9)$$

where

$$A_{ijk} = \frac{1}{2} \int_{V_0} \sigma_{ij} \varepsilon_k \, dV_0 \quad (10)$$

$$A_{ijkl} = \frac{1}{8} \int_{V_0} \sigma_{ij} \varepsilon_{kl} \, dV_0 - \frac{1}{2} \mathbf{u}_{ij} \mathbf{f}_{kl} \quad (11)$$

are the third order and fourth order potential constants, respectively. From the potential energy function the nonlinear equilibrium equations after buckling can be derived. Points of equilibrium are identified by terms of a_i and λ and can be calculated using a stepwise generalized Newton-Raphson scheme. From these data the post-buckling displacement field $\mathbf{u}_{pb}$ can be derived by substitution in equation (5). In case of secondary bifurcation the path of steepest decent is chosen. Summarizing the theory above, the following actions should be taken subsequently when performing this initial post-buckling analysis :

1. Perform a linear elastic analysis
2. Perform an Euler stability analysis
3. Optional plot of buckling modes
4. Selection of relevant modes
5. Solving for the second-order fields
6. Computation of the potential coefficients A_{ijk} and A_{ijkl}
7. Solution of the reduced set of equilibrium equations
8. Optional plots of second-order fields or post-buckling displacement field

3. Discretization

Spline elements are characterized by a spline interpolation function in longitudional direction. These elements have similar properties as flat shell elements, i.e. they can combine plane stress effects with plate bending effects. Spline elements are specially developped for slimline prismatic constructions. These elements must fullfill the following conditions : They must be plane, that is to say, the coordinates of the element nodes must be in one plane. Further, the thickness should be small in relation to the dimension of the element. In addition, spline elements are characterized by the following properties : The basic variables are Cauchy stresses. The displacements perpendicular to the face do not vary along the thickness, and the width of the element in transverse direction is uniform. Finally, the number of nodes in longitudional direction must be specified by the user, where the nodal distribution in longitudional direction is not necessarily equidistantial.

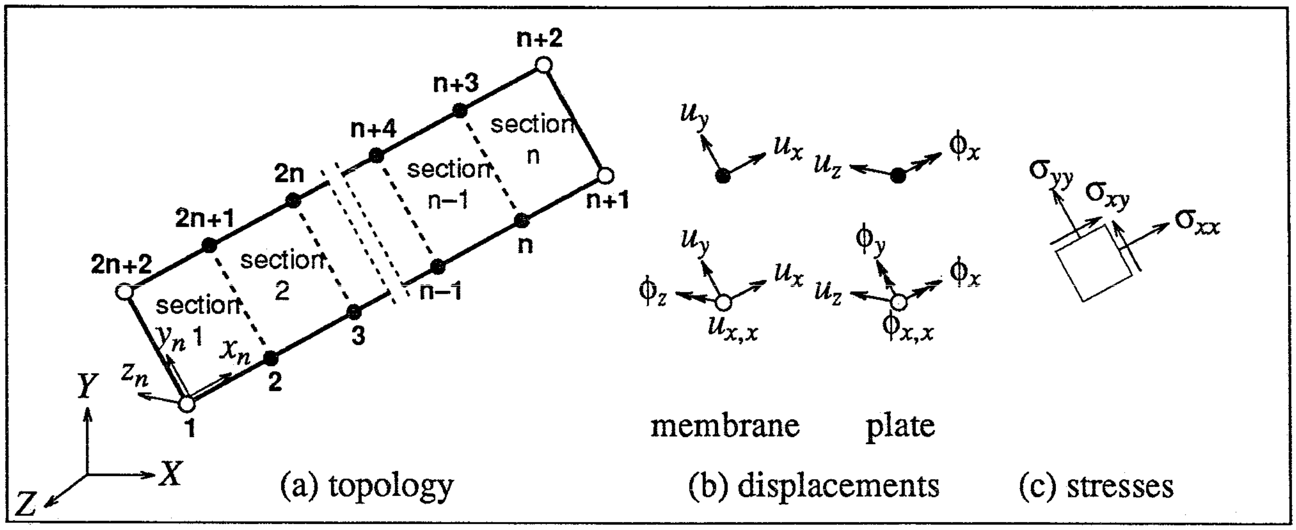

Figure 1 SPLIN2 element

The element is built up from n sections as is shown in the figure 1.

4. Uniform compression of a supported square plate

In this example the buckling and post-buckling behavior of a thin square plate is analyzed.

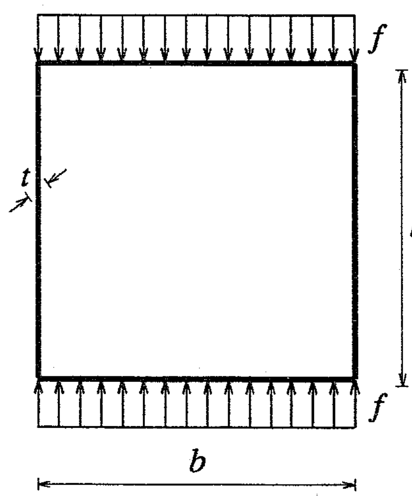

$b = 2000$
$t = 10$
$E = 2\times10^5$
$\nu = 0.3$

Figure 2 Thin plate - Idealized model

As is shown in figure 2 the plate is subjected to a uniform compression. The plate is supported along all the four edges, i.e. no out of plane displacements are allowed at the edges. At the middle points of all four edges the displacements in the direction of the respective edges is also prohibited. This example is derived from the DIANA User's Manual [2]. In the first step the linear elastic solution is calculated (figure 3). Dashed lines represent the undeformed configuration while solid lines concern the deformed plate. In the second step the critical point and the appropriate buckling mode are calculated (figure 4). An analytical solution for the critical load in this problem is given

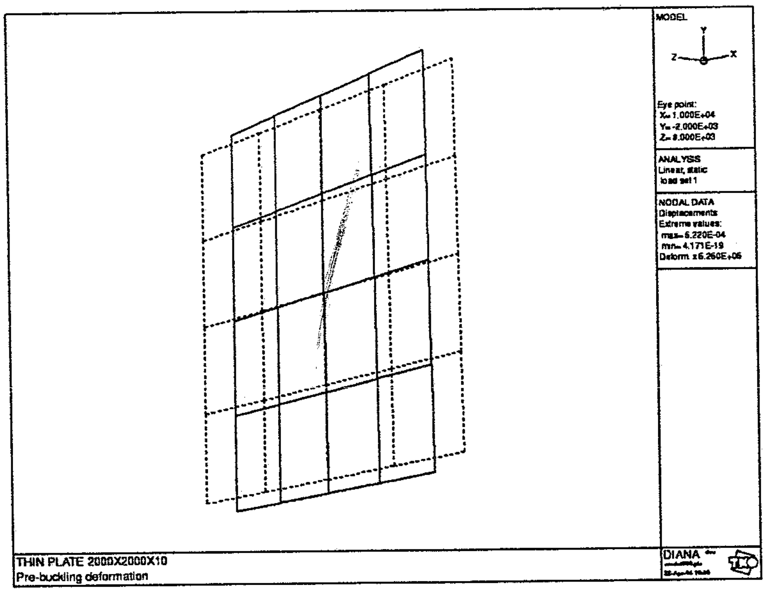

Figure 3 Linear elastic displacements

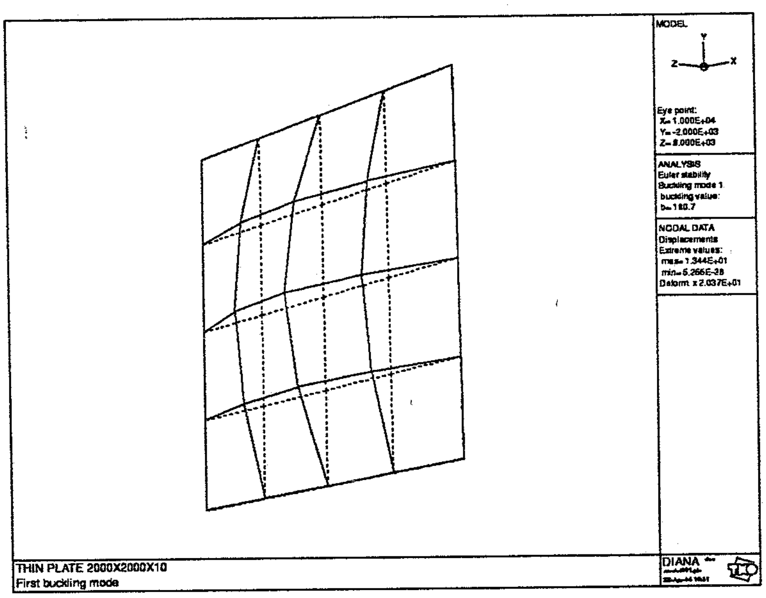

Figure 4 Buckling mode

by Timoshenko and Gere [5] as

$$\lambda^{crit} = \frac{4\pi^2 D}{b^2} \tag{12}$$

with

$$D = \frac{E\,t^3}{12\,(\,1-\nu^2\,)} \tag{13}$$

where b is the length of the plate, E is the Young's modulus, t is the plate thickness and ν is Poisson's ratio. Substituting the actual numerical values for the example yields $\lambda^{crit} = 180.76$ while the calculated value is equal to $\lambda^{crit} = 180.72$. Taking into account the rather course mesh-distribution this is a very acceptable result. In the next step the

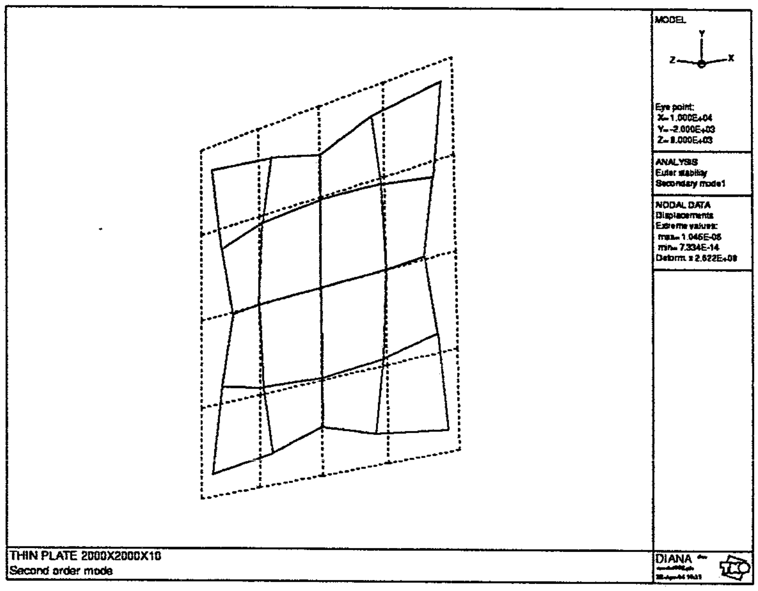

Figure 5 Second-order field

second-order field is calculated, applying a perturbation for only the mode which is shown above. In this case the second-order field is completely in plane. Axial shortening and lateral contraction effects are shown in this mode. In the figures the nodes are connected by straight lines, while in the model these boundaries are smooth spline functions.

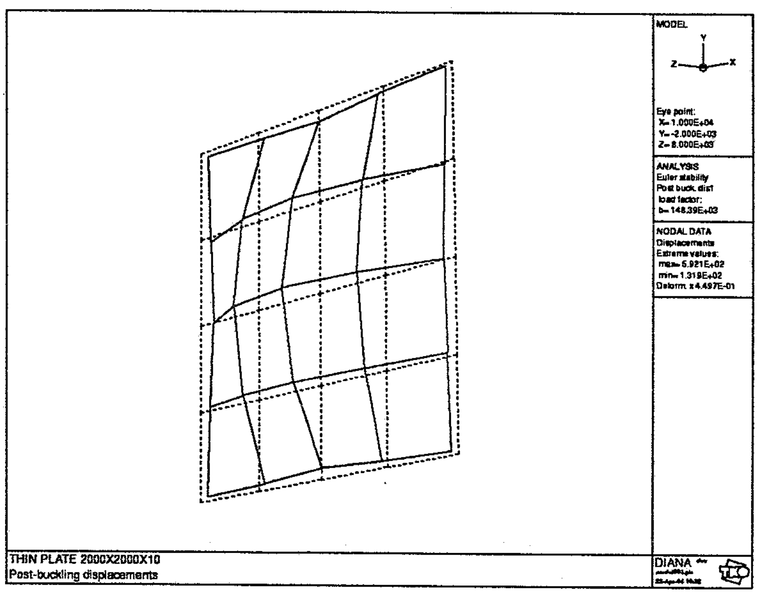

Figure 6 Post-buckling displacements

In the last step the equilibrium path in the post-buckling region is traced. A typical post-buckling displacement field is shown in figure 6, where deformation effects resulting from respectively the linear elastic deformation, the Euler buckling mode and the second-order interaction mode can be recognized.

5. Three point bending of T-beam

In this part the buckling behavior of a simply supported T-beam is studied. The beam is loaded in bending by a concentrated transverse force at mid-span, in such a way that the flange is in compression. As a consequence a nonperiodic buckle may occur locally. For the chosen length and cross-section geometry of the beam in this example, the local and global buckling modes occur at critical points which are very close to each other. Thus, the above mentioned cluster of bifurcation points is present here.

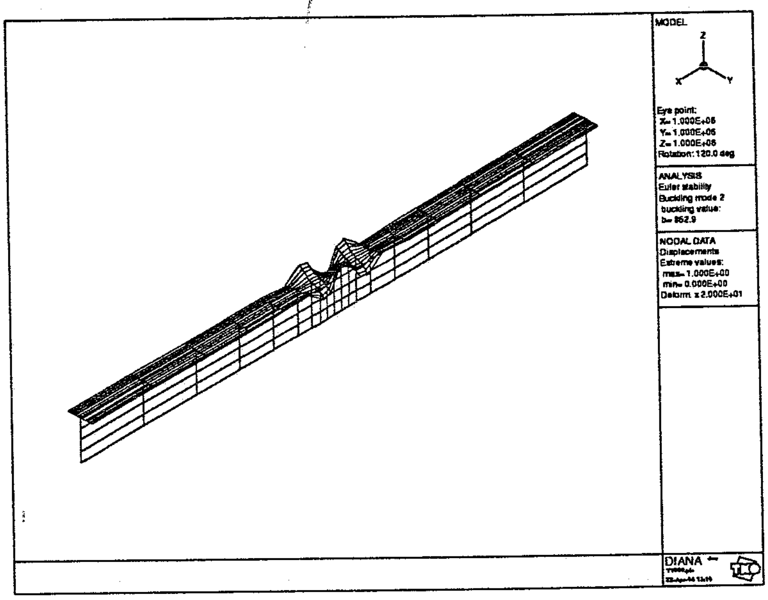

Figure 7 First local buckling mode

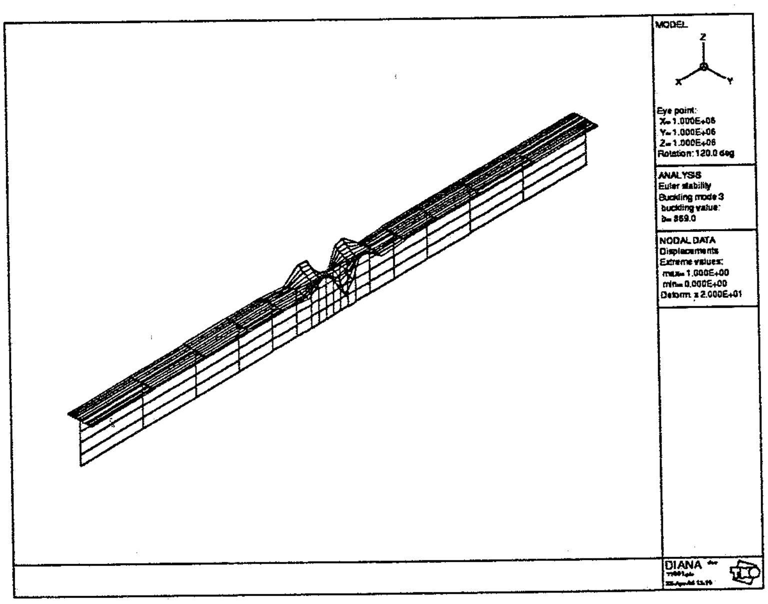

Figure 8 Second local buckling mode

The figures 7 to 9 show a local mode at $\lambda=852.8$, another local mode at $\lambda=868.0$ and the global mode at $\lambda=948.4$, respectively. The perturbation analysis is performed taking these three modes into consideration. The post-buckling equilibrium equations are formulated in terms of the respective amplitudes of these three modes. The strong interaction between the buckling modes in this region is showed by the following.

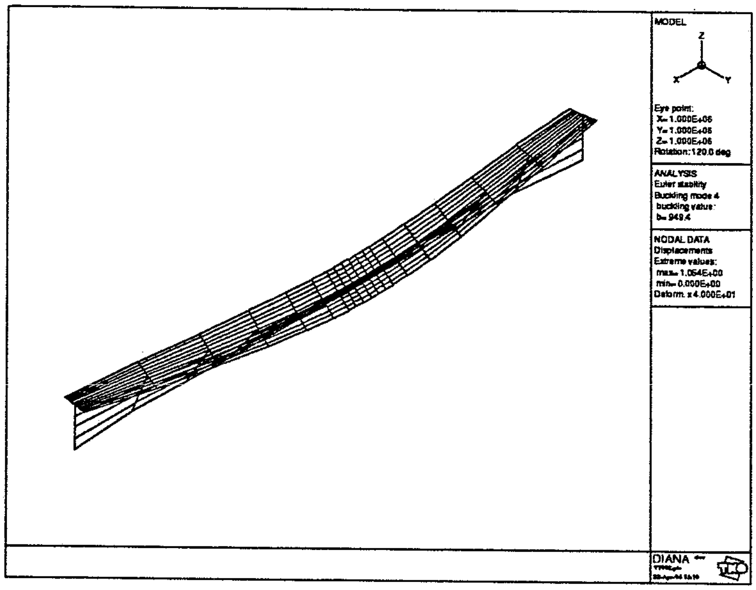

Figure 9 Global buckling mode

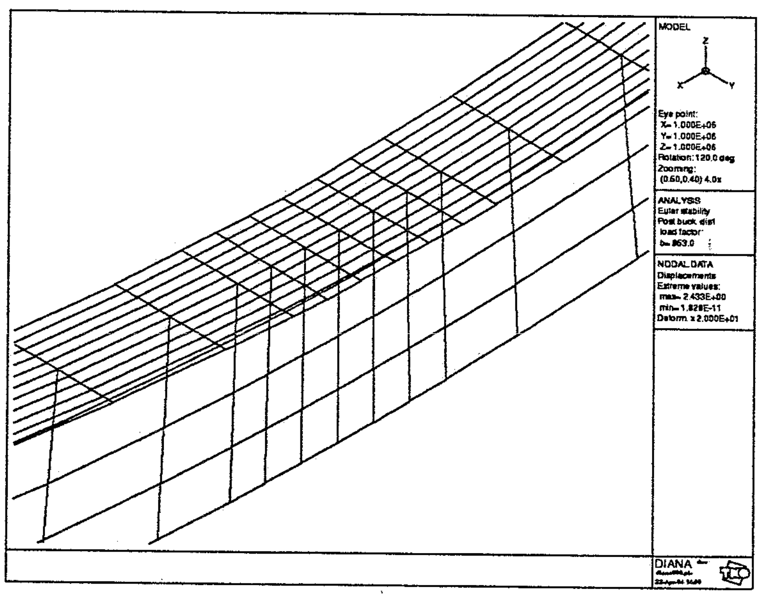

Figure 10 Detail of post buckling deformations after 1 step

In figure 10 the post-buckling displacement field after one step is shown. This point is still very close to the critical point and the deformations are similar to the pre-buckling deformations. Note that the following two figures have the same magnification factor for the displacements than is defined for figure 10. During the first 10 steps the equilibrium path follows the axis for the amplitude of buckling mode 1, while the amplitudes of the modes 2 and 3 stay approximately zero. In this trajectorium the load increases from $\lambda=852.8$ to $\lambda=859.4$ and the web is still plane.

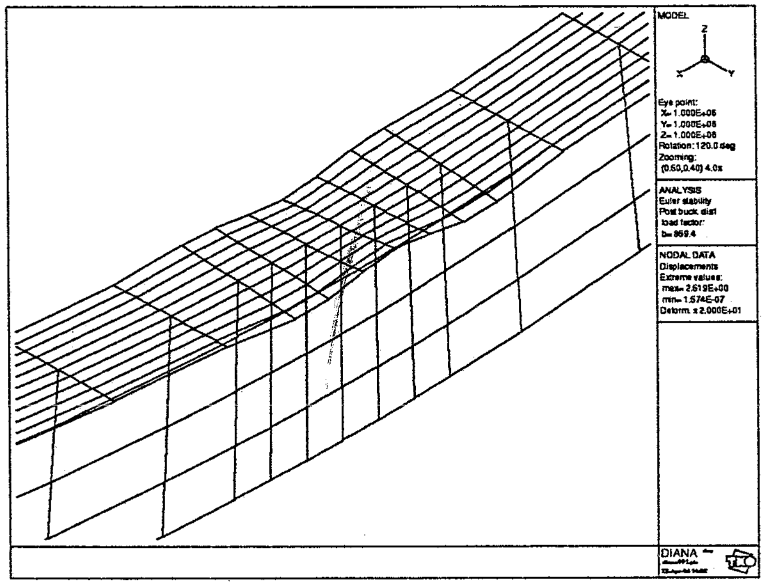

Figure 11 Detail of post buckling deformations after 10 steps

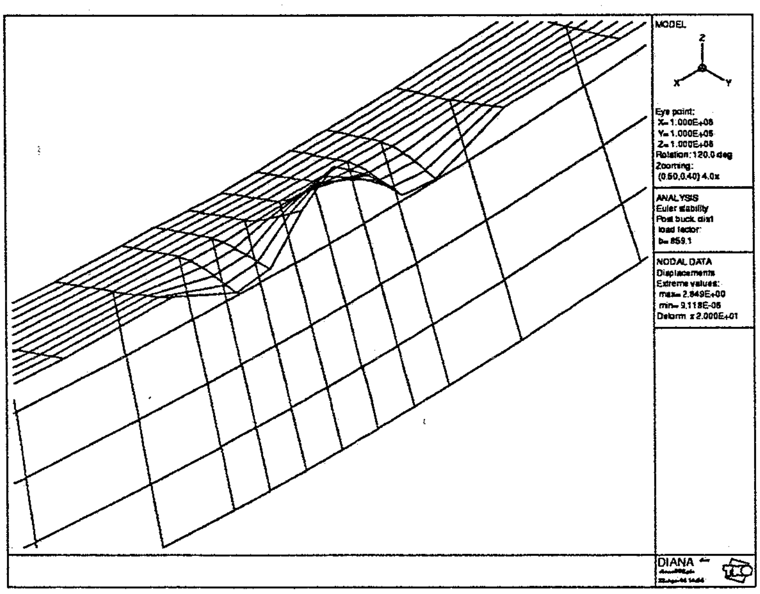

Figure 12 Detail of post buckling deformations after 70 steps

In the 11th step the global buckling mode and the second local buckling mode start to interfere in the post-buckling behavior, and the web is bending side-wards. From this moment the flange is compressed at one side, while it is stretched at the other side. At the stretching side the local buckles are eliminated by the interaction of the second local mode, while at the same time at the compressive side the buckles increase as a result of the interaction by this mode. During side-wards bending movement of the profile, the load initially decreases to $\lambda = 858.0$ and then again increases to $\lambda = 859.2$ at step 70.

6. Conclusions

Application of mode reduction to initial pots-buckling behavior may be a very efficient tool. However, the selection of suitable buckling modes for the perturbation requires a good insight in the mechanical behavior of the structure. Using this analysis tool as a black box is not advised.

ACKNOWLEDGEMENTS

This study is being supported financially by the Technology Foundation (STW) and the Ministry of Transport, Public Works and Water Management (RWS).

REFERENCES

[1]. Byskov, E. and Hutchinson, J.W., Mode interaction in axially stiffened cylindrical shells, AIAA Journal, 15:941-948, 1977.

[2]. DIANA 5.1 User's Manual.

[3]. van Erp, G.M., Advanced buckling analyses of beams with arbitrary cross sections, Thesis Eindhoven University of Technology, 1989.

[4]. Koiter, W.T., Over de stabiliteit van het elastisch evenwicht (in Dutch), Thesis Delft University of Technology, English translation : NASA TT F10, 833, 1967.

[5]. Timoshenko, S.P. and Gere J.M., Theory of Elastic Stability McGraw-Hill, Auckland, 1963.